The Biological Processes of Ferroptosis Involved in Pathogenesis of COVID-19 and Core Ferroptoic Genes Related With the Occurrence and Severity of This Disease

Evolutionary Bioinformatics
Volume 19: 1–13

DOI: 10.1177/11769343231153293
SAGE

Zhengzhong Zhang, Tingting Pang, Min Qi and Gengyun Sun

Department of Respiratory and Critical Care Medicine, The First Affiliated Hospital of Anhui Medical University, Hefei, China.

ABSTRACT

BACKGROUND: A worldwide outbreak of coronavirus disease 2019 (COVID-19) has resulted in millions of deaths. Ferroptosis is a form of iron-dependent cell death which is characterized by accumulation of lipid peroxides on cellular membranes, and is related with many physiological and pathophysiological processes of diseases such as cancer, inflammation and infection. However, the role of ferroptosis in COVID-19 has few been studied.

MATERIAL AND METHOD: Based on the RNA-seq data of 100 COVID-19 cases and 26 Non-COVID-19 cases from GSE157103, we identified ferroptosis related differentially expressed genes (FRDEGs, adj.*P*-value < .05) using the "Deseq2" R package. By using the "clusterProfiler" R package, we performed Gene Ontology (GO) and Kyoto Encyclopedia of Genes and Genomes (KEGG) pathway enrichment. Next, a protein-protein interaction (PPI) network of FRDEGs was constructed and top 30 hub genes were selected by cytoHubba in Cytoscape. Subsequently, we established a prediction model for COVID-19 by utilizing univariate logistic regression and the least absolute shrinkage and selection operator (LASSO) regression. Based on core FRDEGs, COVID-19 patients were identified as two clusters using the "ConsenesusClusterPlus" R package. Finally, the miRNA-mRNA network was built by Targetscan online database and visualized by Cytoscape software.

RESULTS: A total of 119 FRDEGs were identified and the GO and KEGG enrichment analyses showed the most important biologic processes are oxidative stress response, MAPK and PI3K-AKT signaling pathway. The top 30 hub genes were selected, and finally, 7 core FRDEGs (JUN, MAPK8, VEGFA, CAV1, XBP1, HMOX1, and HSPB1) were found to be associated with the occurrence of COVID-19. Next, the two patterns of COVID-19 patients had constructed and the cluster A patients were likely to be more severe.

CONCLUSION: Our study suggested that ferroptosis was involved in the pathogenesis of COVID-19 disease and the functions of core FRDEGs may become a new research aspect of this disease.

KEYWORDS: Coronavirus disease (COVID-19), ferroptosis, biological process, prediction model, RNA network

RECEIVED: November 6, 2022. **ACCEPTED:** January 6, 2023.

TYPE: Original Research

FUNDING: The author(s) received no financial support for the research, authorship, and/or publication of this article.

DECLARATION OF CONFLICTING INTERESTS: The author(s) declared no potential conflicts of interest with respect to the research, authorship, and/or publication of this article.

CORRESPONDING AUTHOR: Gengyun Sun. Department of Respiratory and Critical Care Medicine, The First Affiliated Hospital of Anhui Medical University, 218 Jixi Road, Hefei, Anhui 230022, China. Email: sungengy@126.com

Background

Coronavirus disease 2019 (COVID-19) is an acute infectious respiratory disease caused by severe acute respiratory syndrome coronavirus 2 (SARS-CoV-2).[1] Since December 2019, over 270 million people have been infected with more than 4 million deaths worldwide due to the highly contagious and invasive nature of this virus.[2] Although different types of COVID-19 vaccines candidate in clinical and preclinical development, the variants of the virus may reduce effectiveness of these vaccines.[3] After the SARS-CoV-2 infection, one-fifth of patients may change into severe cases, and the pathologic processes associated with severe COVID-19 include massive type 2 alveolar epithelial cell death, irreversible inflammatory cytokine storm, and impaired immune function.[4]

Ferroptosis, a new type of cell death, is first proposed by Dixon in 2012 and differs from apoptosis and necrosis in terms of execution mechanisms and molecular signaling pathways.[5] Ferrpotosis is mediated by reactive oxygen species, mitochondrial iron metabolism and concentration of lipid peroxidation initiated with enzymatic mechanisms or not.[6,7] The main characteristics of ferroptosis are more integrity of the cell membrane structure than that in apoptosis and necrosis, the decrease and disappearance of mitochodrial cristea which are the prime location of oxidative phosophorylation, and the reduction of GPX4 which is one core enzyme of antioxidant.[7,8] Moreover, Ferroptosis has been implicated in multiple physiological and pathological processes of different diseases, including carcinoma, AKI, neurodegenerative diseases, sepsis, and T-cell immunity.[9]

Recent studies have found that ferroptosis plays a crucial role in many diseases and anti-ferroptosis treatments have become the hotspots. Qi et al[10] revealed that the serum levels of inflammatory factors such as Interleukin 1β (IL-1β), Tumor Necrosis Factor-α (TNF-α) and Interleukin 6 (IL-6)

were significantly higher after being stimulated by RSL-3-a ferroptosis activator.[10] Some ferroptosis-related genes (FRGs) via reprograming the tumor immune microenvironment to enhance tumor cell invasion and growth.[11-13] In addition, ferroptosis has been found to play a profound role in pathogenesis of pulmonary diseases like pneumonia, interstitial lung disease, asthma, and cancer.[14,15] A few studies, however, have examined the relationship between ferroptosis and COVID-19. Thus, we hypothesized that ferroptosis might be involved in the pathogenesis of COVID-19 and that FRGs may participate in its occurrence.

In this study, we surveyed the expression level of FRGs in patients with or not with COVID-19 from GSE157103 and obtained a series of ferroptosis related differentially expressed genes (FRDEGs) between the two group patients. Subsequently, we analyzed the biological function of FRDEGs and constructed the protein-protein interaction (PPI) network of them. Utilized one algorithm of cytoHubba plug-in Cytoscape, top 30 hub genes were chosen for further analysis. Finally, we identified 7 core genes as biomarkers for COVID-19 by combining the expression of hub genes and the clinical date of all patients. Therefore, our study showed the potential mechanism of ferroptosis in the pathogenesis of COVID-19 and highlighted some core FRGs which are related to the occurrence and severity of COVID-19, and these findings could provoke the new insights into the research of COVID-19.

Material and Methods

Data source and processing

Gene expression Omnibus (GEO) is a largest international public repository of high-throughput genomic data and other sequencing data for medical research. In our study, the expression profile and clinical data of GSE157103 were downloaded from GEO. The dataset contains 100 COVID-19 patients and 26 Non-COVID-19 patients. All blood samples were taken from hospitalized patients, and total RNA were extracted for RNA-seq.[16] The flowchat for present research is shown in Figure 1. The "Deseq2" package in R language, a tool for analyzing RNA-seq data, was used to identify the differential expression level of genes in COVID-19 patients compared to Non-COVID-19 patients. Differentially expressed genes (DEGs) were identified with adj.*P*-Val $< .05$ and visualized with volcano plot by the "ggplot2" R package. The 333 genes involving in the process of ferroptosis pathway were identified as ferroptosis related genes (FRGs) from the Molecular Signatures Database (MSigDB, http://www.gsea-msigdb.org/gsea/msigdb/index.jsp). The ferroptosis related differentially expressed genes (FRDEGs) were determined by intersecting the DEGs with FRGs and the Venn diagram were plotted. The heatmap was plotted to show $\log_2$-transformed expression data of FRDEGs using the "pheatmap" R package.

To investigate the biological functions and metabolism-related pathways of FRDEGs, we performed Gene Ontology (GO) and Kyoto Encyclopedia of Genes and Genomes (KEGG) pathway enrichment analyses. GO analyses are used to classify the functions of gene sets in terms of 3 different aspects: biological process (BP), molecular function (MF), and cellular component (CC). Likewise, KEGG pathway enrichment analysis can make a clarity and better view of the functions of gene sets. Briefly, the annotation and enrichment analysis of FRDEGs were performed using the "ClusterProfiler" R package[17] and cut off by $P < .05$. The top 20 results of GO and KEGG analysis were visualized using the "ggplot2" R package. The GO chord was plotted using the "GOplot" R package. A Sankey diagram was plotted using the R package "networkD3" to show the specific FRGs involved in KEGG pathways.

Establishment of PPI network

In order to better understand the interactions between FRDEGs, the PPI network with a cut-off point greater than 0.4 was created using the STRING[18] (https://cn.string-db.org/) online database and visualized by Cytoscape.[19] We used the maximal clique centrality (MCC) algorithm of cytoHubba, a plug-in of Cytoscape, to rank all FRDEGs by degree score and selected top 30 genes as hub genes for further research.[20] In addition, the sub-modules of the PPI network were identified by ClusterONE plugin in Cytosacpe, with a cut-off value of $P < .05$ and the top 3 sub-modules with lowest *P*-value were visualized.

Establishment of a predictive model of COVID-19

Using the 30 hub genes from the PPI network, we utilized univariate logistic regression to identify the link between the level of FRDEGs expression and the occurrence of COVID-19, taking $P < .05$ as the cut-off value. To further select the core genes, the least absolute shrinkage and selection operator (LASSO) regression was used for dimension reduction. The correlation of core genes in prediction of COVID-19 were determined by Spearman correlation analysis using "corrplot" R package. Through the respective coefficient of each core genes, the formula: predictive score = Σ_i expression level of core $\text{gene}_i \times \text{coefficient}_i$ was constructed to calculate the total score of the each sample.

Establishment of the nomogram and validation of predictive model

Based on the core FRDEGs identified above, the nomogram was created to forecast the risk of COVID-19. The "createDataPartition" R function was then used to randomly split all the samples into training (70%) and validation (30%) sets, with a random seed being set to ensure consistency of output after each run of the code. The reliability of the predictive model

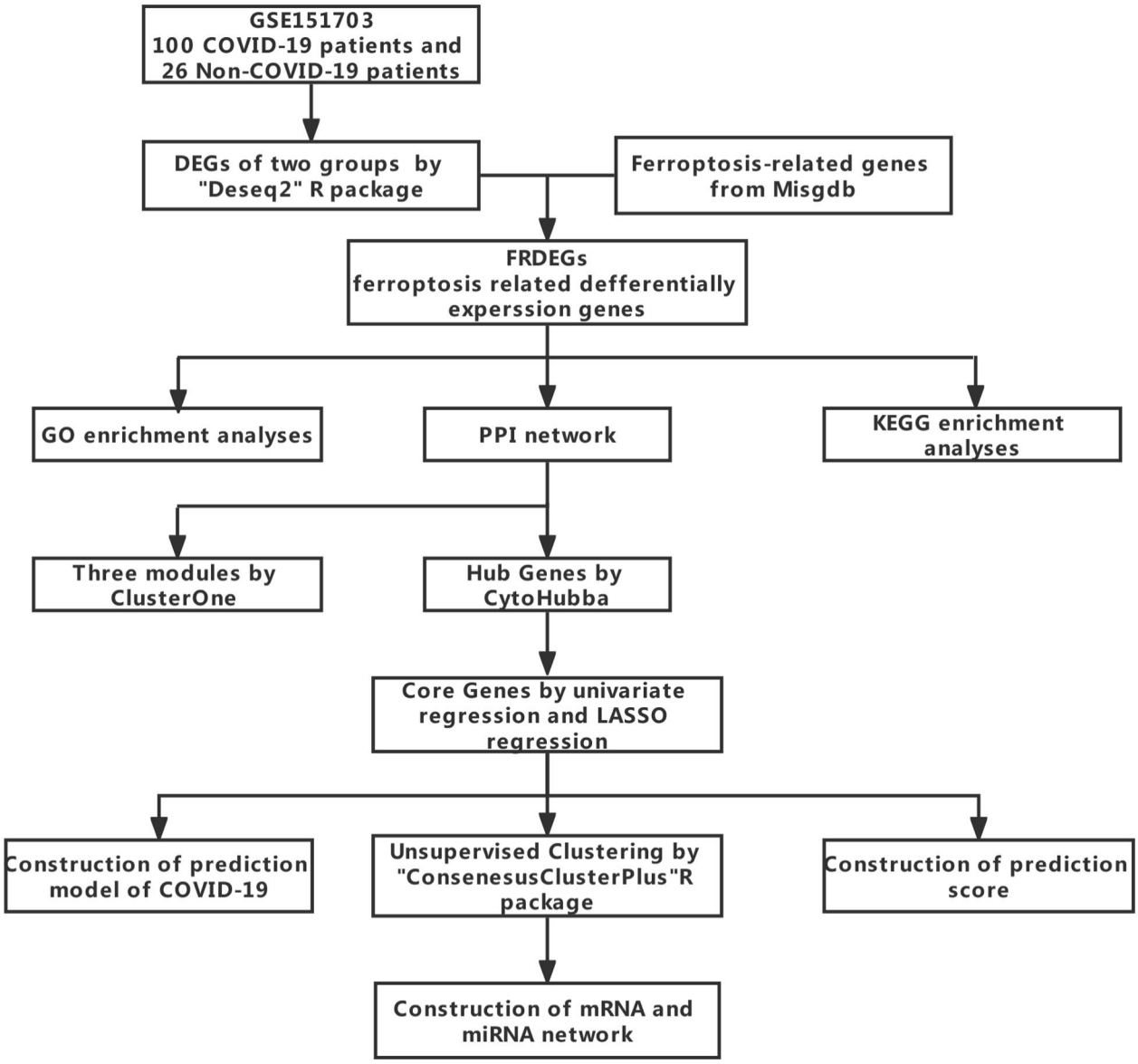

Figure 1. The study flow chart.

constructed by the core genes was assessed by ROC curve in both training and validation sets. Finally, the expression level of core genes in these sets was shown by heatmap using "pheatmap" R package.

Unsupervised clustering of COVID-19 patients

In order to know the subtyping of COVID-19 patients with core genes expression, we performed consensus clustering with K means algorithms using "ConsenesusClusterPlus" R package.[21,22] We visualized The different expression level of core genes and the clinical data in the two cluster patients using "ggplot2" R package.

Establishment of miRNA and mRNA network

Based on the 4 differentially expressed genes between the two clusters, we got the predictive microRNAs (miRNA) which could bind to the messenger (mRNA) using the Targetscan online database (https://www.targetscan.org/vert_72/). Then, the miRNA-mRNA network with the top 5 highest weighted scores were visualized by Cytoscape.

Statistics analysis

All statistical analyses were used a 2-tailed test and $P < .05$ was considered as a significant difference. Relevant analysis is carried out using R software.

Results

FRGs in COVID-19

Comparing the expression level of all genes between the COVID-19 patients and Non-COVID-19 patients from GSE157103, we identified a total of 8145 DEGs, of which 4338 were up-regulated and 3807 were down-regulated (Figure 2A).

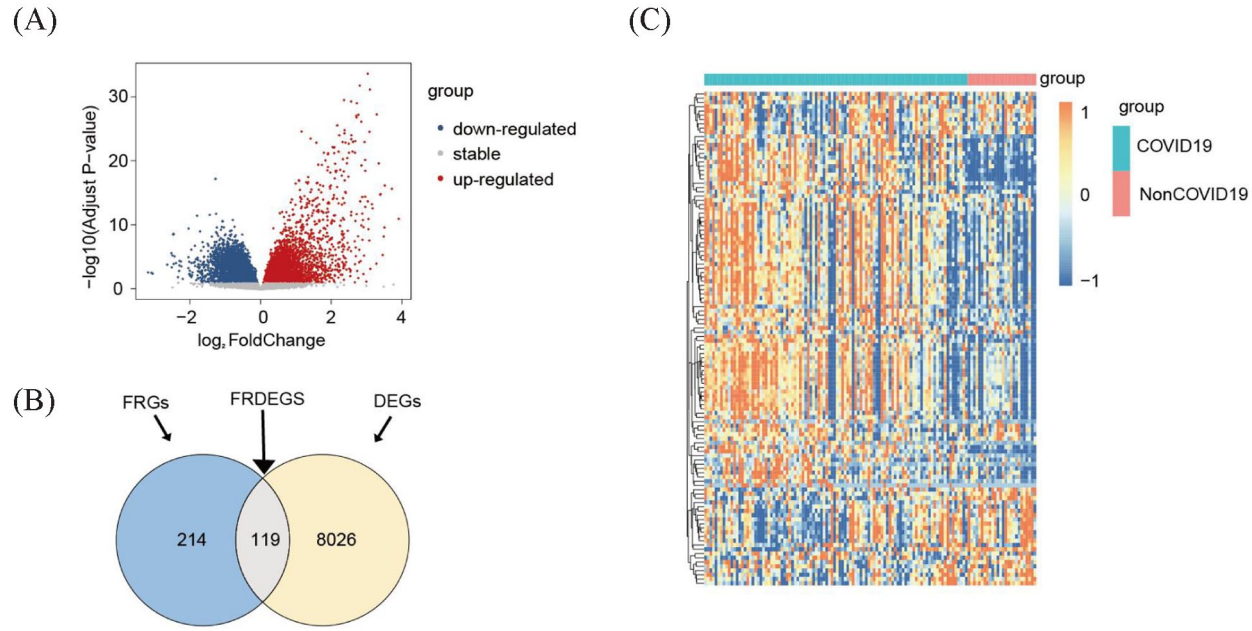

Figure 2. The FRDEGs in GSE157103. (A) The volcano plot, red represents the up-regulated genes, blue represents down-regulated genes, and gray represents stable genes in COVID-19 patients compared with Non-COVID-19 patients. (B) Totally 119 FRDEGs in DEGs. (C) The heatmap of the total FRDEGs in two groups. Blue represents low expression and yellow represents high expression in all samples.
Abbreviations: DEGs, differently expressed genes; FRDEGs, ferroptosis related differently expressed genes; FRGs, ferroptosis related genes.

In order to explore whether there is some correlation between ferroptosis occurred in cell death and the pathogenesis of COVID-19, all DEGs were intersected with FRGs to seek the same genes. As shown in the Venn diagram, a total of 119 FRDEGs were discovered (Figure 2B). In addition, among the FRDEGs we found, 75 of them were up-regulated and the rest were down-regulated in COVID-19 patients' blood cells. Then heatmap of the FRDEGs expression in the two groups was exhibited (Figure 2C), and it was clear that there are differences between the patients with or not with COVID-19 on the level of some FRGs expression.

GO and KEGG enrichment analyses of FRDEGs

According to GO analysis, the biological functions of FRDEGs were engaged in oxidative stress, outer mitochondrial membrane metabolism, and protein kinase activation (Figure 3A). All of these are crucial steps in cell injury and metabolic disturbances.[23] We showed the specific genes associated with top 10 BP processes by GO cord plot and found that the up-regulated expression genes (CAV1, MYB, EPAS and ATF3) were implicated in oxidative stress and neuronal death, while the down-regulated expression genes (HSPB1, HBA1, HMOX1 and EGLN2) were involved in cellular responses to stresses from chemical and external (Figure 3B). The KEGG enrichment analysis showed most FRDEGs were significantly involved in autophagy, lipid and atherosclerosis, apoptosis, mitophagy, spinocerbellar ataxia, human T-cell leukemia virus 1 infection, MAPK signaling pathway and PI3K-Akt signaling pathway (Figure 3C), for additional details see in Supplemental Table S1. Sankey diagram was depicted to show some important signaling pathways such as apoptosis, autophagy, lipid and atherosclerosis with its explicit genes (Figure 3D).

The PPI network and modules of FRDEGs

Using STRING database to get PPI network of the FRDEGs, we selected top 30 genes with highest correlation coefficient scores as hub genes by cytohubba for subsequent research (Figure 4A). In addition, the core network modules from the constructed PPI network were identified by ClusterONE in Cytosacpe software. The lower the *P*-value for each module, the higher the polymerization energy and the link between the functions of proteins in the module. Finally, 3 modules with lowest *P*-value (module one: $P = 1.1 \times 10^{-9}$; module two: $P = 2.5 \times 10^{-8}$; module 3: $P = .01$) were showed respectively, and each of them contain most of hub genes we selected (Figure 4B–D).

Construction of COVID-19 predictive model

To examine the pathogenesis of the hub genes in COVID-19 patients, a series of bioinformatic analysis were utilized. First, we used univariate logistic regression to determine which hub gene is influenced the occurrence of COVID-19, and then selected 15 relative genes by a *P*-value less than .05 (Table 1). Subsequently, LASSO regression was applied for feature selection and deeply screening of these 15 genes. In 10-fold cross-validation, lambda-min was considered the best choice (Figure 5A and B), and 7 core genes with their respective

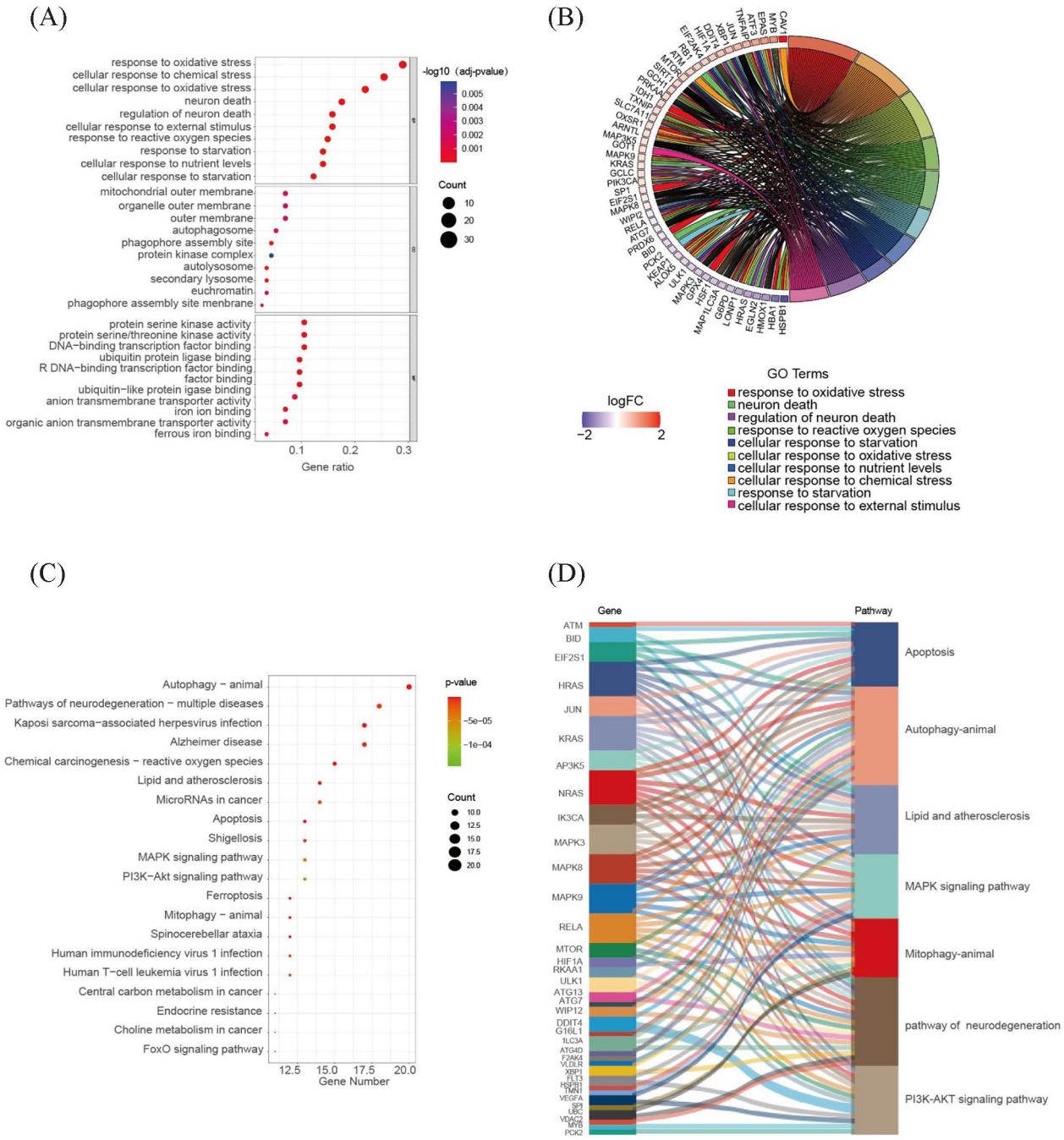

Figure 3. KEGG and GO enrichment process of FRDEGs. (A) The bubble diagram of GO enrichment analysis. Top 10 of each GO process (BP、MF and CC) are shown in the diagram. (B) The top 10 biological processes of FRDEGs are shown by GO cord, blue represents down-regulated genes and red represents up-regulated genes. (C) Top 20 pathways by KEGG enrichment of FRDEGs are shown by bubble diagram. (D) Sankey diagram of KEGG enrichment analysis and its specific FRDEGs.
Abbreviations: BP, biological processing; CC, cellular component; MF, molecular function.

regression coefficients were obtained. The expression of these core genes were significantly different between COVID-19 and Non-COVID-19 patients ($P < .05$). It was found that HMOX1 and HSPB1 were down-regulated, and the other 5 genes (JUN, MAPK8, VEGFA, CAV1, XPB1) were up-regulated (Figure 5C), and the high expression level of HMOX1 and HSPB1 in Non-COVID-19 patients suggested that HMOX1 and HSPB1 were probably be protective factors for COVID-19. Additionally, the correlation of the core genes was examined, and their pattern was mapped (Figure 5D). The results showed that CAV1 had the strongest positive correlation with XBP1 (coefficient = .86), while MAPK8 had the strongest negative correlation with HSPB1 (coefficient = −0.32). Finally, we constructed the predictive scores of

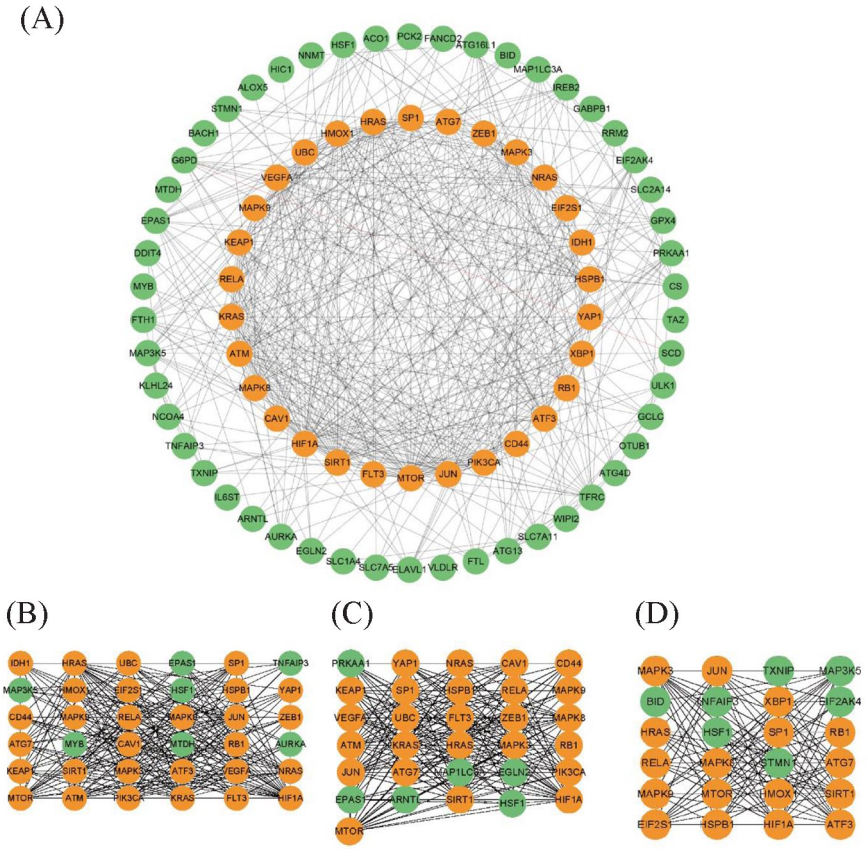

Figure 4. The PPI Network of FRDEGs. (A) The interleaved circle diagrams show the protein-related interaction relationships of proteins encoded by FRDEGs. The score of each FRDEGs were calculated according to the MCC algorithm, and the inner circle represents top 30 FRDEGs while the remaining genes to form the outer circle. (B–D) Top 3 clusters of PPI network by ClutsterONE. Yellow represents the top 30 genes by MCC algorithm, green represents the rest genes.

Table 1. Univariate logistic regression of FRDEGs in the occurrence of COVID-19.

FRDEGS	*R* VALUE	*P* VALUE
JUN	1.11	.01
MAPK8	−2.25	.02
HRAS	−0.94	0
KRAS	0.9	.08
HIF1A	0.96	.01
VEGFA	1.77	.02
RB1	1.26	.01
NRAS	1.83	.02
SP1	1.44	.01
HMOX1	−1.61	0
IDH1	1.13	.01
CAV1	1.96	.02
XBP1	1.93	0
HSPB1	−0.92	0

core genes in COVID-19 patients using the results of LASSO regression (Table 2), and the scores of COVID-19 patients were significantly higher compared to that in Non-COVID-19 patients (Figure 5E).

Validation of the core genes in COVID-19 patients

The normgram was plotted according to the expression level of each core gene and the regression coefficient in the patients with and without COVID-19 (Figure 6A). The ROC curve was used to test the application value of the constructed model, and AUC for the training and validation sets were 0.953 and 0.897, indicating the high accuracy of the constructed model (Figure 6B and C). Moreover, the ROC curve of each core genes in the occurrence of COVID-19 was shown in Figure 7. As a whole, the AUC range for the core genes was 0.665 to 0.804, with XBP1 having the highest AUC at 0.804 and MAPK8 having the lowest at 0.673. This suggested that the core genes identified in this study might play an important role in COVID-19 patients and are involved in the pathological process of COVID-19. Subsequently, heat maps of the core genes were plotted separately in both training set and validation set, showing that they were significantly differentially

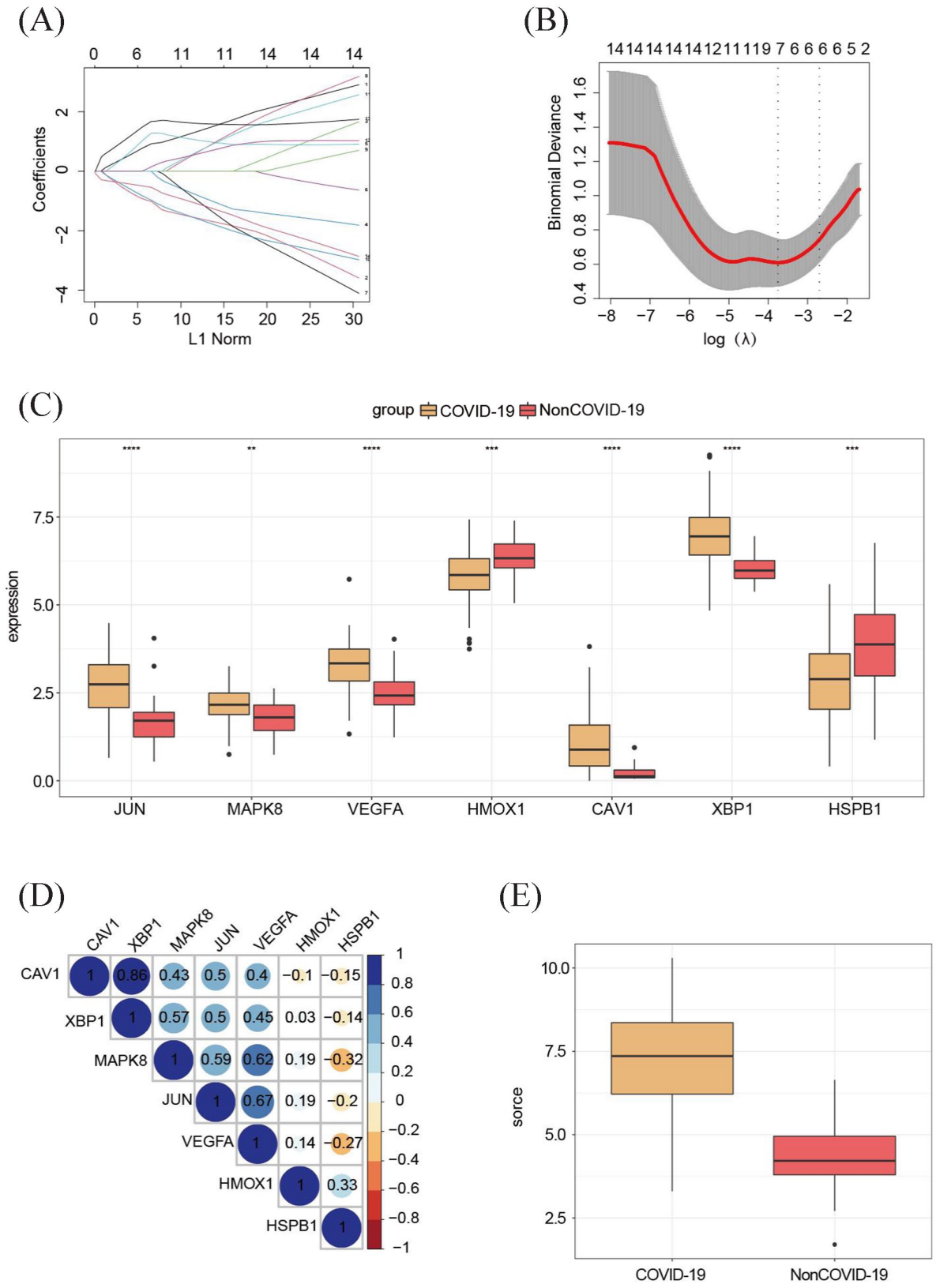

Figure 5. Characterization of core genes associated with COVID-19 in FRDEGs. (A) Least absolute shrinkage and selection operator (LASSO) coefficient profiles of COVID-19 related FRDEGs. (B) LASSO regression by 10-fold cross-validation to choose the best tuning parameter. (C) Box plot shows the expression levels of core genes in COVID-19 patients compared with Non-COVID-19 patients. (D) Correlation plot of 7 core genes in all samples. Blue represents positive correlation while red represents negative correlation between the core genes. The magnitude of the correlation coefficient is represented by the numbers in the circles. (E) Box plot shows the scores of constructed core genes between COVID-19 patients and Non-COVID19 patients.

Table 2. Correlation coefficient of 7 core genes by LASSO regression.

GENE	COEFFICIENT
JUN	0.779
MAPK8	−0.925
VEGFA	1.030
HMOX1	−0.828
CAV1	0.006
XBP1	1.489
HSPB1	−0.493

expressed in COVID-19 patients compared to Non-COVID-19 patients (Figure 6D and E).

Deferent patterns of COVID-19 patients

Based on the 7 core genes identified above, COVID-19 patients were divided into cluster A and cluster B by a consistent clustering algorithm (Figure 8A). We observed that the two clusters were different in predictive scores, and the expression levels of JUN, MAPK8, CAVI, and XBP1 were significantly higher in cluster B patients compared to those in cluster A patients (Figure 8B and C). Moreover, there was a significantly greater likelihood for cluster A patients to require mechanical ventilation, be admitted to the intensive care unit (ICU), or have complications related to diabetes mellitus (DM) compared to cluster B patients (Figure 8D and E). According to these results, severe COVID-19 might be related to high expression levels of JUN, MAPK8, CAVI, and XBP1.

The miRNA-mRNA network of core genes

Through the differentially expressed genes between two clusters of COVID-19 patients, we predicted miRNAs which could bind to its mRNAs using the targetscan database and mapping the network in Cytoscape according to the top 5 weighted congtext score (Figure 9). Surprisingly, miR-199-5p is a same predicted target for both CAV1 and XBP1 in the ceRNA network, this could theoretically explain the positive correlation of expression between the 2 genes, however this speculation needs to be confirmed experimentally.

Discussion

COVID-19 epidemic is a serious threat to people's health, posing significant socioeconomic burden.[24] Additionally, a portion of the hospitalized COVID-19 patients may suffer post-COVID-19 sequelae such as fatigue, depression, dyspnea.[25] There are limited medical intervention strategies to prevent the COVID-19.[26] Therefore, the deeper we clarify the pathogenic mechanisms of this disease, the better treatment efficacy will be. Emerging evidence indicated that the multi-organ failures rapidly happened in severe COVID-19 cases may due to the hemoglobin damage which could lead to iron overload.[27,28] However, it is unclear whether ferroptosis which has iron metabolism disorder is involved in the aggravation of COVID-19.

At the molecular level, disease-related genes have distinct transcription and translation in different physiological or pathological states of the same cell type.[29] Thus, in order to investigate the interrelationship of ferroptosis and COVID-19, we identified FRDEGs through intersecting the DEGs with FRGs. The function and regulation of FRDEGs might have a potential and crucial role in COVID-19. One biological process identified by GO enrichment analysis of FRDEGs in our study, oxidative stress, had been shown to increase within cells after infections with various viruses, such as the human respiratory syncytial virus, rhinoviruses, and influenza virus.[30-32] Moreover, recent studies have shown that the accumulation of oxidative stress in endothelium cells aggravates the severity and mortality of COVID-19.[33,34] KEGG enrichment analysis of FRDEGs indicated that the PI3K-AKT signaling pathway and MAPK signaling pathway might be involved in the pathogenesis of COVID-19. PI3K-AKT signaling pathway, a magnifying singling cascade regulated by protein phosophprylation and dephosphorylation, is activated after patients who were infected with SARS-COV-2 to enhance autophagy, apoptotic and inflammation in endothelial cells.[35] Apoptosis signal-regulating kinase 1 (ASK1), a member of the MAP3K family, can be activated by erastin, a ferroptosis inducer compound, to promote cell death and inflammatory response.[36,37] Therefore, it is worthwhile to demonstrate in the future whether the FRDEGs via these biologic processes or pathways take part in the occurrence and development of COVID-19.

In this study, PPI network diagram of FRDEGs showed the specific top 30 FRDEGs we had chosen for further research. The most selected FRDEGs were contained in top 3 modules via ClusterONE algorithm, suggesting that in some extent they are valuable for research. Finally, we established the prediction model containing 7 core FRDEGs (JUN, MAPK8, VEGFA, CAV1, XBP1, HMOX1, and HSPB1). Coincidentally, functions of some core genes were closely associated with the development of COVID-19. HMOX1 protein plays an anti-inflammatory role to attenuate serious conditions such as sepsis, tissue injury and fibrinogenesis, all of which are damaged to our healthy after bacterial infection as well as SARS-CoV-2 infection.[38] By using spectrometry analysis, it is possible to determine that the human HMOX1 protein can bind to the SARS-CoV-2 open reading frame 3 a (ORF3a), which can then directly activate the NLPR3 inflammasome pathway to create the inflammation storm which is thought to be one driving factor of ARDS.[39,40] Moreover, another protective gene against COVID-19 we have found is HSPB1, the coding protein of which has an extracellular anti-inflammation function.[41] Therefore, recent studies are consistent with our findings that

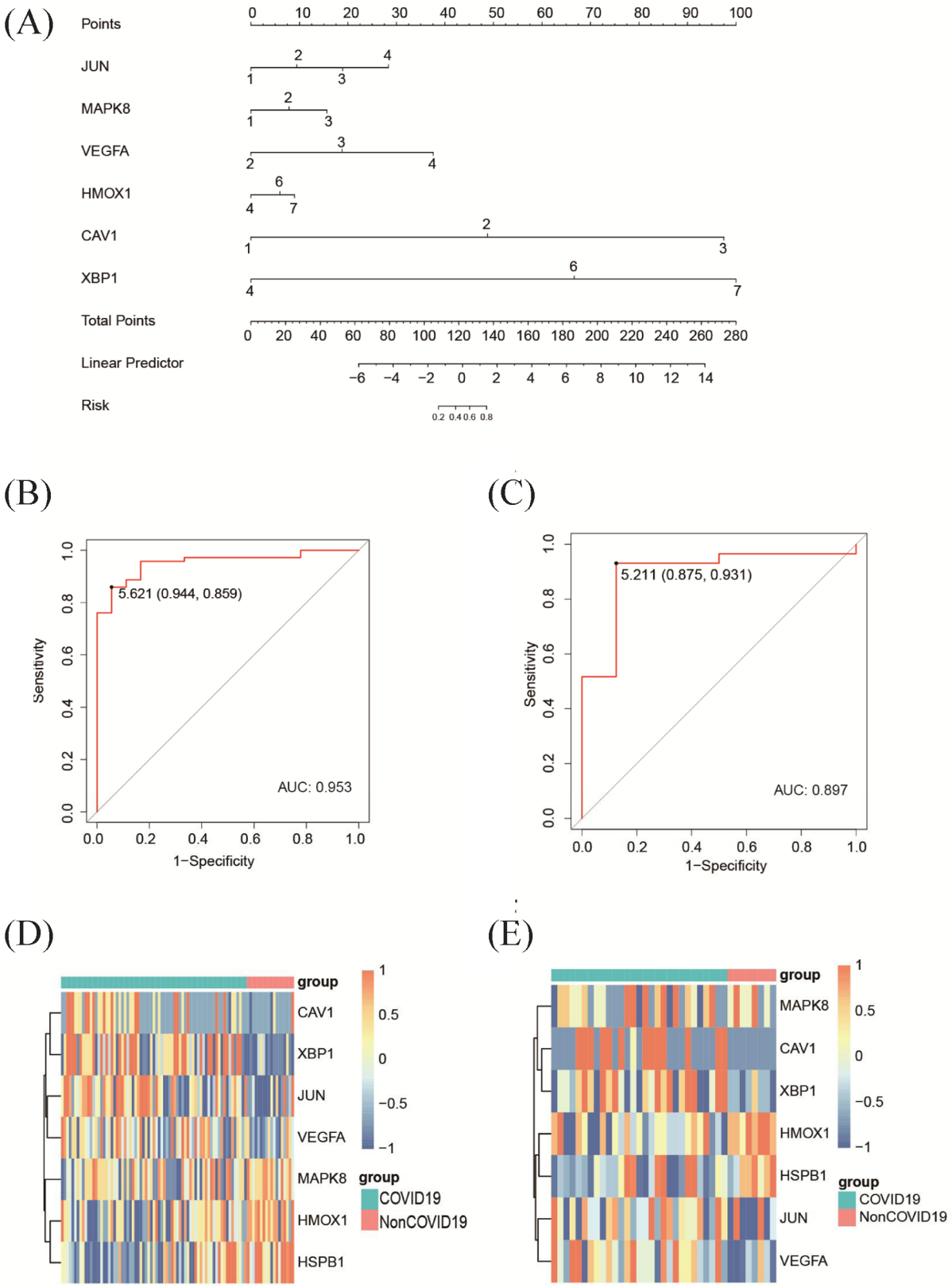

Figure 6. Identification of core genes from FRDEGs in COVID-19. (A) Normgram of core genes which are related with the risk of occurrence of COVID-19. (B and C) ROC curves for the predictive evaluation of 7 core genes in the training and validation sets and the area under the respective curves. (D and E) The heatmap of 7 core genes expression in the training set and the validation set.

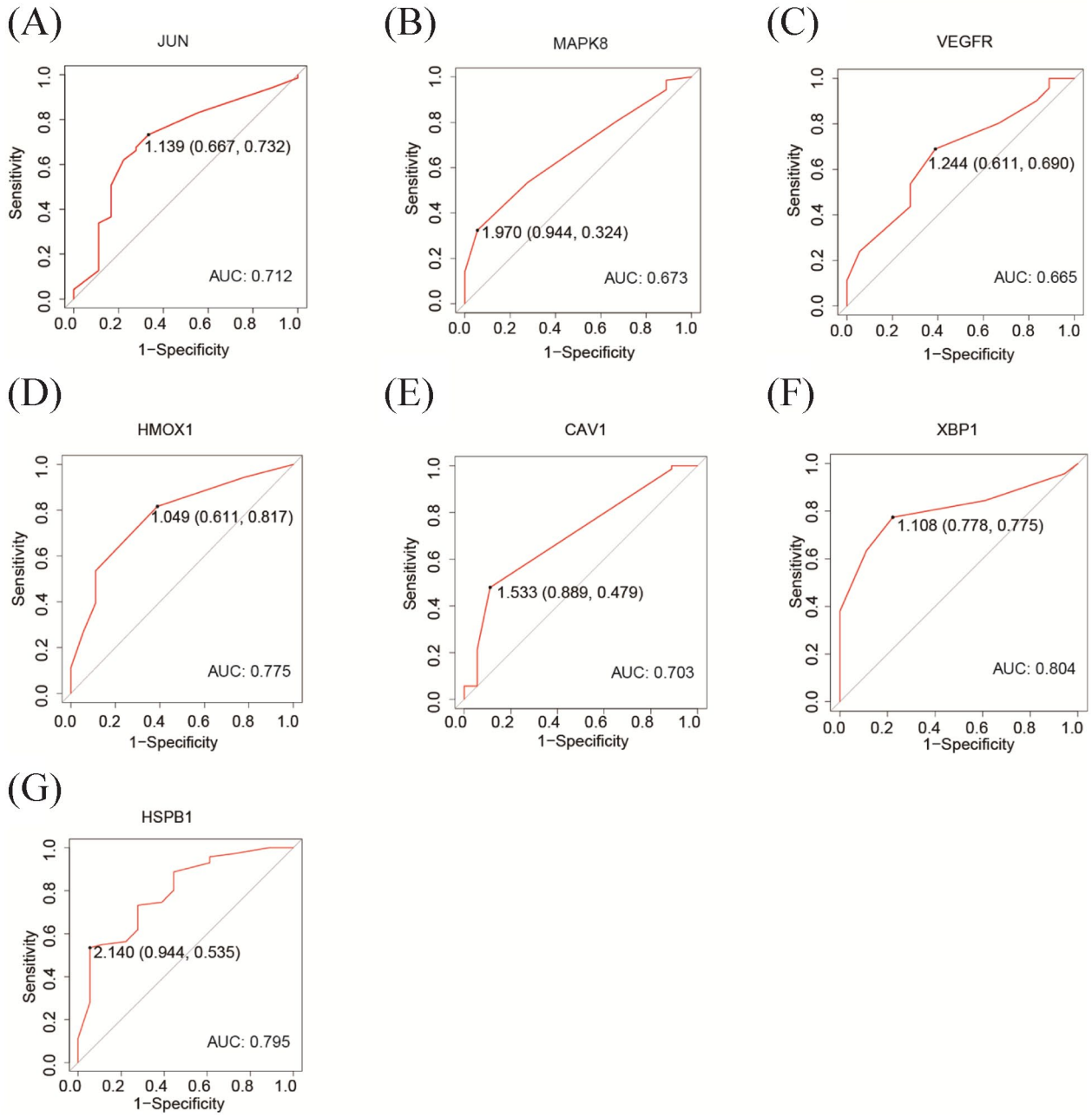

Figure 7. ROC curves of each core genes. (A-G) The ROC curves show the diagnostic value of each core genes in the occurrence of COVID-19.

one of protective factor for COVID-19 patients may be the high expression levels of HMOX1 and HSBP1. In addition to HSPB1 and HMOX1, other core genes are also critical in the pathogenesis of virus-associated diseases. JNKs, a group of MAPKs containing MAPK8, target JUN which is a member of the activator protein 1 (AP1), and the activation of AP1 can cause a variety of effects, including cell death after influenza A virus infection, migration and differentiation of tumor cells.[42,43] Furthermore, as a major marker of caveolae in endothelial cells, CAV1 are increasing expressed by HIV infection and also interacts with a lot of intracellular signaling molecules such as MAPK and VEGFA.[44-46] Therefore, the real functions of these core genes in COVID-19 patients are worthy of investigating and validating in the future.

The prediction model we constructed by FRDEGs showed high AUC value in both training and validation sets. However, the accuracy and practicability of the model need to be further investigated. Additionally, patients had COVID-19 were classified into two clusters with the expression level of core genes. We found that cluster A COVID-19 patients have a higher proportion of ICU admission, ventilator treatment and DM than cluster B patients, indicating that cluster A patients are more severe. It is also indicated that DM can down-regulate the innate immunity function to make worse severity and

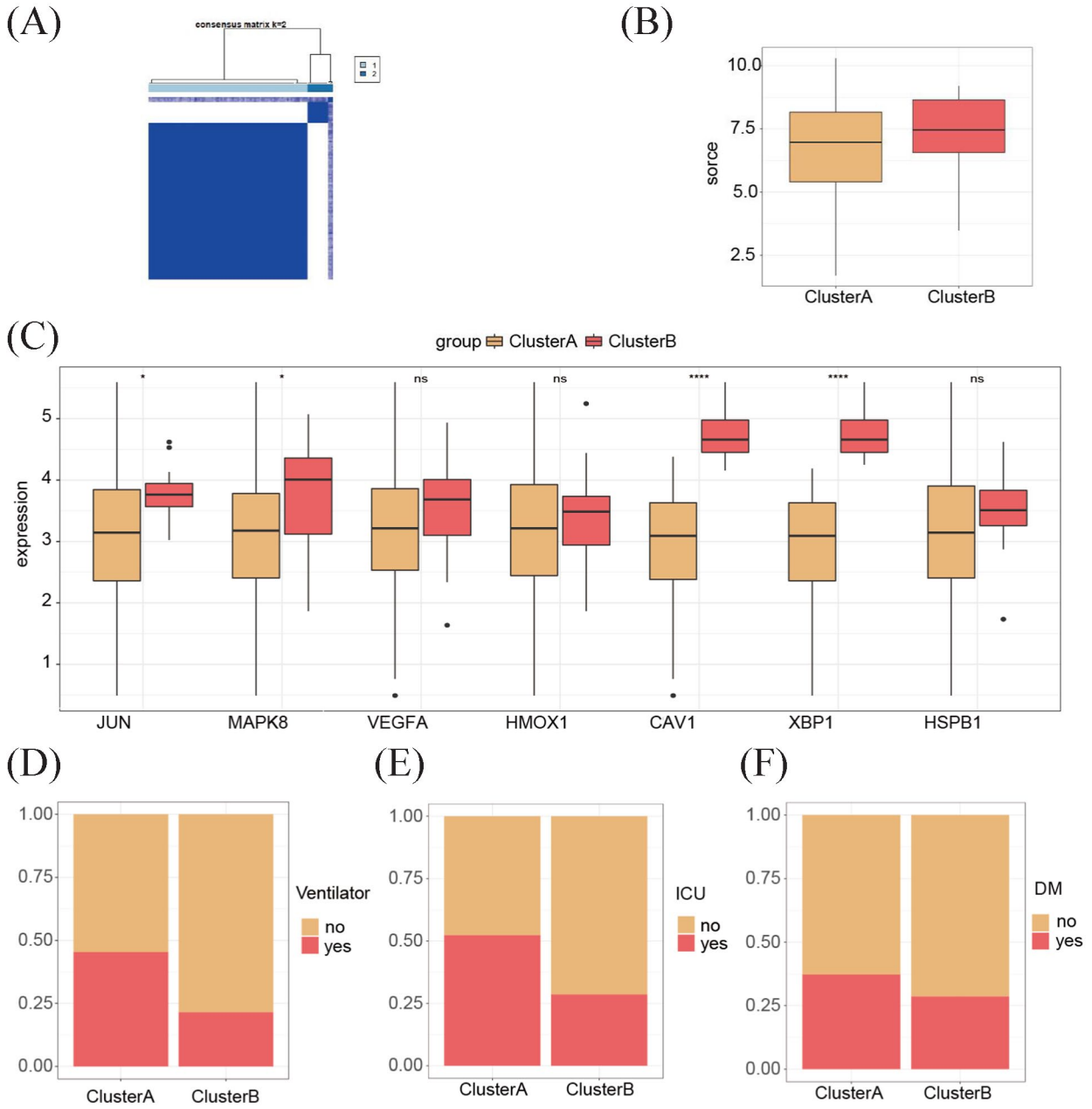

Figure 8. Two clusters of COVID-19 patients and the different clinical syndrome. (A) The unsupervised clustering of COVID-19 patients by core genes and the best rank is $k=2$. (B) The prediction scores of core genes between two clusters. (C) Box plot of expression status of core genes in different clusters. (D–F) Differences in clinically important indicators between the two cluster patients.

fatality of COVID-19 patients.[47] Moreover, we found 4 core genes (XBP1, MAPK8, CAV1, JUN) which had different expression level between the two clusters patients. These 4 genes with a higher expression levels in cluster A might be the driving factors of severe COVID-19 cases. The miRNAs, one type of non-coding RNAs, have been found to be epigenetic regulators by binding to their target mRNAs and then suppressing the expression of mRNAs.[48] According to recent studies, there have been demonstrated that some miRNAs can affect the translation of their target mRNAs, such as MiR-199 can down-regulate the expression of XBP1[49] and MiR-451 can bind CAV1 to alleviate the proliferation of gliobalstoma.[50] Therefore, to find the regulator relationship of miRNA will be better to discover the functions of core gene and cure the COVID-19 patients.[51]

There are some limitations of our research. First, additional clinical samples are necessary to confirm the expression level of FRGs and the value of prediction model of COVID-19 patients. Furthermore, due to the quarantine management and higher infectious rate of COVID-19 patients, it is difficult for

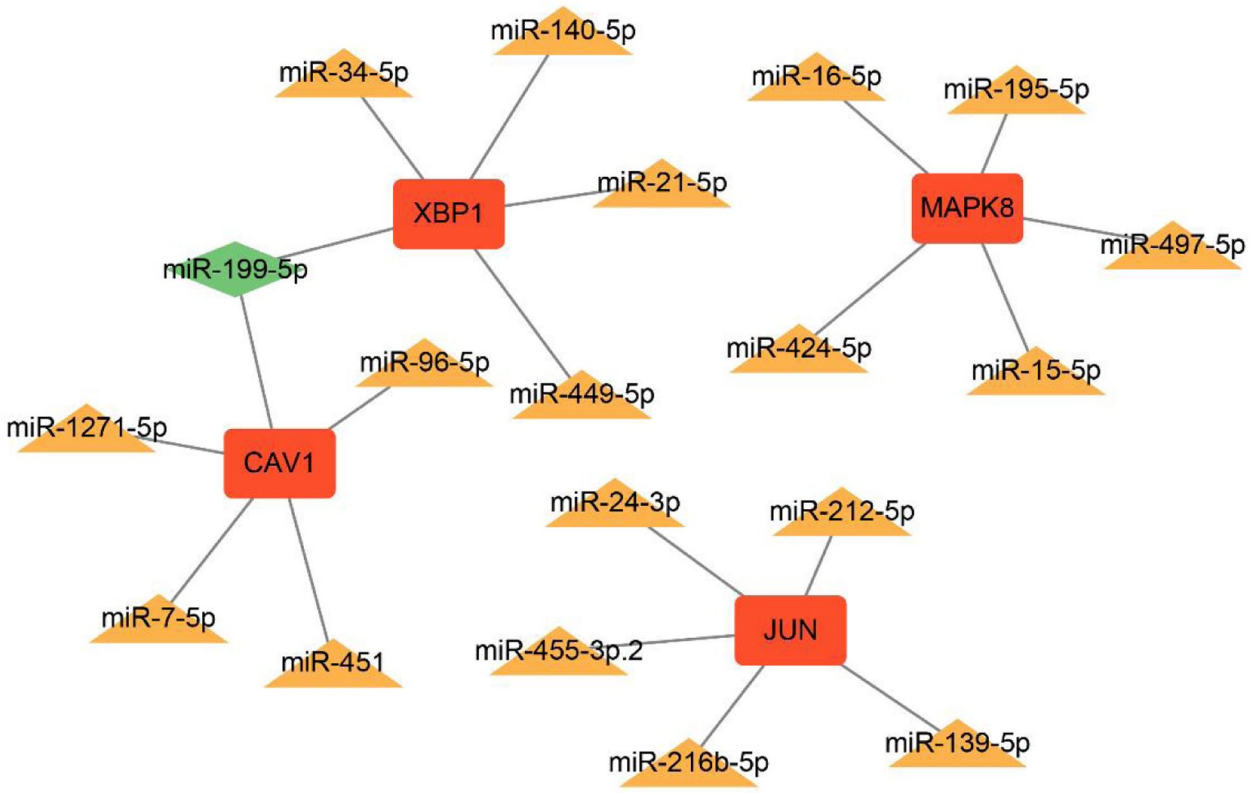

Figure 9. The miRNA-mRNA network. Red rectangle represents the mRNA of 4 differentially expression genes in two clusters, yellow triangle represents the predicted miRNA, green diamond represents miRNA which can bind to different mRNA.

us to get blood samples to validate the true expression level and biological process of FRDEGs in COVID-19.

Conclusions

This study revealed the correlation between the ferroptosis and COVID-19 infection and indicated the important biological processes and signaling pathways which the FRDEGs may involve in. The predictive model based on 7 core FRDEGs was constructed and was to show a high accuracy. The COVID-19 patients can be divided into two clusters by core genes, and the cluster A patients were inclined to severe cases. Finally, we constructed RNAs network with the different expression of core genes in two clusters. However, the molecular mechanisms of core FRDEGs in COVID-19, as well as the functions of miRNAs remain to be confirmed in the future experimental studies.

Acknowledgements

We acknowledge GEO database for providing their platforms and contributors for uploading their meaningful datasets.

Author Contributions

Zhengzhong Zhang and Gengyun Sun contributed to the study conception and design. Data collection and analysis were performed by Zhengzhong Zhang, Tingting Pang, Min Qi. The first draft of the manuscript was written by Zhengzhong Zhang and all authors commented on previous versions of the manuscript. All authors read and approved the final manuscript.

ORCID iD

Zhengzhong Zhang https://orcid.org/0000-0001-9478-2338

Supplemental Material

Supplemental material for this article is available online.

REFERENCES

1. Chen Y, Klein SL, Garibaldi BT, et al. Aging in COVID-19: Vulnerability, immunity and intervention. *Ageing Res Rev*. 2021;65:101205.
2. To KK, Sridhar S, Chiu KH, et al. Lessons learned 1 year after SARS-CoV-2 emergence leading to COVID-19 pandemic. *Emerg Microbes Infect*. 2021;10:507-535.
3. Chung JY, Thone MN, Kwon YJ. COVID-19 vaccines: the status and perspectives in delivery points of view. *Adv Drug Deliv Rev*. 2021;170:1-25.
4. Ochani R, Asad A, Yasmin F, et al. COVID-19 pandemic: from origins to outcomes. A comprehensive review of viral pathogenesis, clinical manifestations, diagnostic evaluation, and management. *Infez Med*. 2021;29:20-36.
5. Liu P, Feng Y, Li H, et al. Ferrostatin-1 alleviates lipopolysaccharide-induced acute lung injury via inhibiting ferroptosis. *Cell Mol Biol Lett*. 2020;25:10.
6. Stockwell BR, Friedmann Angeli JP, Bayir H, et al. Ferroptosis: A regulated cell death Nexus linking metabolism, redox biology, and disease. *Cell*. 2017;171:273-285.
7. Dixon SJ, Lemberg KM, Lamprecht MR, et al. Ferroptosis: an iron-dependent form of nonapoptotic cell death. *Cell*. 2012;149:1060-1072.
8. Yang Y, Luo M, Zhang K, et al. Nedd4 ubiquitylates VDAC2/3 to suppress erastin-induced ferroptosis in melanoma. *Nat Commun*. 2020;11:433.
9. Sun Y, Chen P, Zhai B, et al. The emerging role of ferroptosis in inflammation. *Biomed Pharmacother*. 2020;127:110108.
10. Qi J, Kim JW, Zhou Z, Lim CW, Kim B. Ferroptosis affects the progression of nonalcoholic steatohepatitis via the modulation of lipid peroxidation-mediated cell death in mice. *Am J Pathol*. 2020;190:68-81.
11. Wu Y, Zhang S, Gong X, et al. The epigenetic regulators and metabolic changes in ferroptosis-associated cancer progression. *Mol Cancer*. 2020;19:39.

12. Wang X, Chen Y, Wang X, et al. Stem cell factor SOX2 confers ferroptosis resistance in lung cancer via upregulation of SLC7A11. Cancer Res. 2021;81:5217-5229.
13. Chen P, Wu Q, Feng J, et al. Erianin, a novel dibenzyl compound in Dendrobium extract, inhibits lung cancer cell growth and migration via calcium/calmodulin-dependent ferroptosis. *Signal Transduct Target Ther.* 2020;5:51.
14. Xu W, Deng H, Hu S, et al. Role of ferroptosis in lung diseases. *J Inflamm Res*. 2021;14:2079-2090.
15. Cheng H, Feng D, Li X, et al. Iron deposition-induced ferroptosis in alveolar type II cells promotes the development of pulmonary fibrosis. *Biochim Biophys Acta Mol Basis Dis*. 2021;1867:166204.
16. Overmyer KA, Shishkova E, Miller IJ, et al. Large-scale multi-omic analysis of COVID-19 severity. *medRxiv*. Jul 19 2020. doi:10.1101/2020.07.17.20156513
17. Yu G, Wang LG, Han Y, He QY. clusterProfiler: an R package for comparing biological themes among gene clusters. *OMICS*. 2012;16:284-287.
18. Szklarczyk D, Gable AL, Nastou KC, et al. The STRING database in 2021: customizable protein-protein networks, and functional characterization of user-uploaded gene/measurement sets. *Nucleic Acids Res*. 2021;49:D605-D612.
19. Kohl M, Wiese S, Warscheid B. Cytoscape: software for visualization and analysis of biological networks. *Methods Mol Biol*. 2011;696:291-303.
20. Chin CH, Chen SH, Wu HH, Ho CW, Ko MT, Lin CY. CytoHubba: identifying hub objects and sub-networks from complex interactome. *BMC Syst Biol*. 2014;8:S11.
21. Wilkerson MD, Hayes DN. ConsensusClusterPlus: a class discovery tool with confidence assessments and item tracking. *Bioinformatics*. 2010;26:1572-1573.
22. Brière G, Darbo É, Thébault P, Uricaru R. Consensus clustering applied to multi-omics disease subtyping. *BMC Bioinformatics*. 2021;22:361.
23. Naviaux RK. Metabolic features of the cell danger response. *Mitochondrion*. 2014;16:7-17.
24. Kim Y, Gordon A, Rowerdink K, Herrera Scott L, Chi W. The impact of the COVID-19 pandemic on health care utilization among insured individuals with common chronic conditions. *Med Care*. 2022;60:673-679.
25. Nalbandian A, Sehgal K, Gupta A, et al. Post-acute COVID-19 syndrome. *Nat Med*. 2021;27:601-615.
26. Uchikov A, Paunov L, Batashki A, et al. Surgical treatment of pneumothorax in patients with COVID-19 - results and management. *Folia Med (Plovdiv)*. 2021;63:663-669.
27. Ganz T, Aronoff GR, Gaillard CAJ, et al. Iron Administration, infection, and anemia management in CKD: untangling the effects of intravenous Iron therapy on immunity and infection risk. *Kidney Med*. 2020;2:341-353.
28. Zhou F, Yu T, Du R, et al. Clinical course and risk factors for mortality of adult inpatients with COVID-19 in Wuhan, China: a retrospective cohort study. *Lancet*. 2020;395:1054-1062.
29. Xiang J, Zhang NR, Zhang JS, Lv XY, Li M. PrGeFNE: predicting disease-related genes by fast network embedding. *Methods*. 2021;192:3-12.
30. Buffinton GD, Christen S, Peterhans E, Stocker R. Oxidative stress in lungs of mice infected with influenza A virus. *Free Radic Res Commun*. 1992;16:99-110.
31. Wang MM, Lu M, Zhang CL, et al. Oxidative stress modulates the expression of toll-like receptor 3 during respiratory syncytial virus infection in human lung epithelial A549 cells. *Mol Med Rep*. 2018;18:1867-1877.
32. Footitt J, Mallia P, Durham AL, et al. Oxidative and nitrosative stress and histone deacetylase-2 activity in exacerbations of COPD. *Chest*. 2016;149:62-73.
33. Chernyak BV, Popova EN, Prikhodko AS, Grebenchikov OA, Zinovkina LA, Zinovkin RA. COVID-19 and oxidative stress. *Biochemistry*. 2020;85:1543-1553.
34. Delgado-Roche L, Mesta F. Oxidative stress as key player in Severe Acute Respiratory syndrome coronavirus (SARS-CoV) infection. *Arch Med Res*. 2020;51:384-387.
35. Khezri MR. PI3K/AKT signaling pathway: a possible target for adjuvant therapy in COVID-19. *Hum Cell*. 2021;34:700-701.
36. Hattori K, Ishikawa H, Sakauchi C, Takayanagi S, Naguro I, Ichijo H. Cold stress-induced ferroptosis involves the ASK1-p38 pathway. *EMBO Rep*. 2017;18:2067-2078.
37. Ichijo H, Nishida E, Irie K, et al. Induction of apoptosis by ASK1, a mammalian MAPKKK that activates SAPK/JNK and p38 signaling pathways. *Science*. 1997;275:90-94.
38. Batra N, De Souza C, Batra J, Raetz AG, Yu AM. The HMOX1 pathway as a promising target for the treatment and prevention of SARS-CoV-2 of 2019 (COVID-19). *Int J Mol Sci*. 2020;21:6412.
39. Gordon D, Jang G, Bouhaddou M, et al. A SARS-CoV-2 protein interaction map reveals targets for drug repurposing. *Nature*. 2020;583:459-468.
40. Chen IY, Moriyama M, Chang MF, Ichinohe T. Severe Acute Respiratory Syndrome coronavirus viroporin 3a activates the NLRP3 inflammasome. *Front Microbiol*. 2019;10:50.
41. Batulan Z, Pulakazhi Venu VK, Li Y, et al. Extracellular release and signaling by heat shock protein 27: role in modifying vascular inflammation. *Front Immunol*. 2016;7:285.
42. Zhang J, Ruan T, Sheng T, et al. Role of c-Jun terminal kinase (JNK) activation in influenza A virus-induced autophagy and replication. *Virology*. 2019;526:1-12.
43. Sun Y, Liu WZ, Liu T, Feng X, Yang N, Zhou HF. Signaling pathway of MAPK/ERK in cell proliferation, differentiation, migration, senescence and apoptosis. *J Recept Signal Transduct Res*. 2015;35:600-604.
44. Mergia A. The role of Caveolin 1 in HIV infection and Pathogenesis. *Viruses*. 2017;9:129.
45. Zou M, Huang W, Jiang W, Wu Y, Chen Q. Role of Cav-1 in HIV-1 Tat-induced dysfunction of tight junctions and Aβ-Transferring proteins. *Oxid Med Cell Longev*. 2019;2019:3403206.
46. Puddu A, Sanguineti R, Maggi D. Caveolin-1 down-regulation reduces VEGF-A secretion induced by IGF-1 in ARPE-19 cells. *Life*. 2021;12:44.
47. Wu J, Zhang J, Sun X, et al. Influence of diabetes mellitus on the severity and fatality of SARS-CoV-2 (COVID-19) infection. *Diabetes Obes Metab*. 2020;22:1907-1914.
48. Pu M, Chen J, Tao Z, et al. Regulatory network of miRNA on its target: coordination between transcriptional and post-transcriptional regulation of gene expression. *Cell Mol Life Sci*. 2019;76:441-451.
49. Lou Z, Gong YQ, Zhou X, Hu GH. Low expression of miR-199 in hepatocellular carcinoma contributes to tumor cell hyper-proliferation by negatively suppressing XBP1. *Oncol Lett*. 2018;16:6531-6539.
50. Wang Y, Lin Z, Song J, et al. MicroRNA-451a targets caveolin-1 in stomach cancer cells. *Int J Clin Exp Pathol*. 2020;13:2524-2533.
51. Buruiană A, Florian ȘI, Florian AI, et al. The roles of miRNA in glioblastoma tumor cell communication: diplomatic and aggressive negotiations. *Int J Mol Sci*. 2020;21:1950.